ISSN 1674-1056
http://cpb.iphy.ac.cn
http://iopscience.iop.org/cpb
中国物理 B
Chinese Physics
中国物理 Chinese Physics B

Microparticle collection for water purification based on laser-induced convection

Zhi-Hai Liu(刘志海), Jiao-Jie Lei(雷皎洁), Yu Zhang(张羽), Ya-Xun Zhang(张亚勋), Xing-Hua Yang(杨兴华), Jian-Zhong Zhang(张建中), Yun Yang(杨军), Li-Bo Yuan(苑立波)
Citation: Chin. Phys. B . 2018, 27(5): 054210. **doi:** 10.1088/1674-1056/27/5/054209

Journal homepage: http://cpb.iphy.ac.cn; http://iopscience.iop.org/cpb

What follows is a list of articles you may be interested in

Cavity optomechanics: Manipulating photons and phonons towards the single-photon strong coupling

Yu-long Liu(刘玉龙), Chong Wang(王冲), Jing Zhang(张靖), Yu-xi Liu(刘玉玺)
Chin. Phys. B . 2018, 27(2): 024204. **doi:** 10.1088/1674-1056/27/2/024204

Angular-modulated spatial distribution of ultrahigh-order modes assisted by random scattering

Xue-Fen Kan(阚雪芬), Cheng Yin(殷澄), Tian Xu(许田), Fan Chen(陈凡), Jian Li(李建), Qing-Bang Han(韩庆邦), Xian-Feng Chen(陈险峰)
Chin. Phys. B . 2017, 26(11): 114210. **doi:** 10.1088/1674-1056/26/11/114210

Control of microwave signals using bichromatic electromechanically induced transparency in multimode circuit electromechanical systems

Cheng Jiang(江成), Yuanshun Cui(崔元顺), Xintian Bian(边心田), Xiaowei Li(李晓薇), Guibin Chen(陈贵宾)
Chin. Phys. B . 2016, 25(5): 054204. **doi:** 10.1088/1674-1056/25/5/054204

Stationary entanglement between two nanomechanical oscillators induced by Coulomb interaction

Qin Wu(吴琴), Yin Xiao(肖银), Zhi-Ming Zhang(张智明)
Chin. Phys. B . 2016, 25(1): 014203. **doi:** 10.1088/1674-1056/25/1/014203

Multiple optical trapping based on high-order axially symmetric polarized beams

Zhou Zhe-Hai, Zhu Lian-Qing
Chin. Phys. B . 2015, 24(2): 028704. **doi:** 10.1088/1674-1056/24/2/028704

Lasing properties of a Yb ion in tetragonal $LuPO_4$ and $LuVO_4$ isomorphic crystals: A comparative study*

Xiao-Dan Dou(窦晓丹), Jing-Nan Yang(杨婧男), Jie He(贺杰), Li-Sha Wang(王丽莎), Wen-Juan Han(韩文娟), Hong-Hao Xu(徐洪浩), De-Gao Zhong(钟德高), Bing Teng(滕冰), and Jun-Hai Liu(刘均海)†

College of Physics, Qingdao University, Qingdao 266071, *China*

(Received 20 December 2017; revised manuscript received 18 January 2018; published online 26 April 2018)

A comprehensive investigation is carried out to compare the spectroscopic properties, absorption saturation behaviors and lasing properties of a Yb ion in tetragonal $LuPO_4$ and $LuVO_4$ isomorphic crystals. Significant distinctions are revealed in many aspects of the lasing behavior for the Yb ion doped in the two crystal hosts, and Yb:$LuPO_4$ proves to be superior to Yb:$LuVO_4$ since it enables efficient laser action to be much more easily achieved. With a 0.6 mm thick crystal plate of Yb:$LuPO_4$, an output power of 3.30 W can be generated with an optical–optical conversion efficiency of 50.8%; whereas with a 2 mm long miniature crystal rod, the output power produced can reach 8.35 W with an optical–optical conversion efficiency of 46.7%.

Keywords: Yb ion, lasing properties, $LuPO_4$ crystal, $LuVO_4$ crystal

PACS: 42.55.Rz, 42.60.Pk, 42.55.Xi **DOI:** 10.1088/1674-1056/27/5/054210

1. Introduction

The trivalent ytterbium (Yb) ion has become one of the most useful active ions that can be doped into host media to constitute various laser materials. It has a very simple electronic configuration, possessing only two electronic states in the optical transition regime, that is, the ground state $^2F_{7/2}$ and an excited state $^2F_{5/2}$. This feature makes it advantageous over the traditional Nd ion that has been widely used in the 1-μm spectral region, because detrimental effects, such as concentration quenching, energy transfer and up-conversion, can be largely diminished.

Among the wide varieties of host crystals that have been developed thus far for the Yb ion, those of tetragonal zircon structures belonging to the space group $I4_1/amd$ and point group $4/mmm$ are of particular significance. These include orthovanadates and orthophosphates. The orthovanadates, including YVO_4, $GdVO_4$ and $LuVO_4$, have been recognized as a class of most important host crystal for trivalent lanthanide active ions, in particular for the most common Nd ion.[1] As host medium for Yb ion, these orthovanadate crystals prove to be also unique in that the laser action of Yb ion exhibits optical bistability.[2,3] Unlike orthovanadates that can be easily grown from melt by the conventional Czochralski method, the orthophosphates are not congruently melting and can only, up to now, be grown by the high-temperature solution method. The difficulty in growing large-size crystal of high optical quality has greatly hampered the development of laser materials based on orthophosphates, although they have long been known to be promising host crystals for trivalent lanthanide active ions.[4] In fact, it was not until 2014 that the first laser action of Yb ion in orthophosphates was demonstrated with a Yb:$LuPO_4$ crystal plate.[5] Since then, progress has been made in growing miniature columnar crystals of Yb:$LuPO_4$, as well as in studies of its continuous-wave (CW) and Q-switched laser performance.[6–9]

Given the isomorphic crystal structures of $LuPO_4$ and $LuVO_4$ and the identical lattice site having a local symmetry of point group D_{2d} at which the Yb ion enters, it will be interesting and instructive to compare the lasing properties of Yb ion in these two host crystals in order to clarify how and to what extent the host crystal structure and ligand field (crystal field) can determine the basic lasing properties of an active ion.

In this paper, we report on our results from such a comprehensive investigation into the basic lasing properties of Yb ion in the two host crystals. We first make a detailed comparison of the spectroscopic properties. Then the saturation behavior of absorption for pumping radiation is discussed in some detail. After that, the lasing properties are compared for two cases with emitting laser beam parallel to the a or c crystallographic axis.

2. Experiment

The crystal of Yb ion-doped $LuVO_4$ (Yb:$LuVO_4$) was grown by the Czochralski method, with a Yb ion concentration of 1.5 at.% (1.96×10^{20} cm^{-3}). The crystal samples utilized were cut along a or c crystallographic axis (a-cut or c-cut), each with a square aperture of 3.3 mm×3.3 mm and a

*Project supported by the National Natural Science Foundation of China (Grant No. 11574170).

†Corresponding author. E-mail: junhai_liu@hotmail.com

© 2018 Chinese Physical Society and IOP Publishing Ltd

thickness of 2.0 mm. The Yb ion-doped $LuPO_4$ (Yb:$LuPO_4$) was grown in high-temperature solution from spontaneous nucleation, with a Yb ion concentration of 5.0 at.% (6.15×10^{20} cm^{-3}). Two crystal samples were used in this experiment: a 0.6 mm thick crystal plate with thickness along its crystallographic a axis (aperture of 3.0 mm×5.0 mm) and a 2.0 mm long miniature columnar crystal rod (along c axis) with a transverse dimension of about 0.7 mm. The end faces of the Yb:$LuVO_4$ samples and the Yb:$LuPO_4$ miniature rod were carefully polished, whereas the Yb:$LuPO_4$ crystal plate was unpolished. For all the crystal samples, no antireflection coatings were placed on their end faces.

To study the lasing properties of the Yb ion in these two host crystals, we employed a simple plano-concave resonator, as illustrated schematically in Fig. 1. The plane mirror, M1, was coated for high transmittance ($> 95\%$) at a pumping wavelength of 976 nm and for high reflectance at 1010–1100 nm ($> 99.5\%$) where lasing occurs. The concave mirror, M2, having a radius of curvature $R_2 = 15$ or 25 mm, was used as an output coupler of the laser oscillator and its transmittance (output coupling T) could be chosen in a wide range from $T = 0.5\%$ to $T = 60\%$. To achieve an efficient laser action, the crystal plate sample was fixed on a copper heat-sink, whereas other crystal samples were fitted into a copper holder. Both copper heat-sinks were maintained at a temperature of 5 °C by cooling water. In order to examine the lasing properties of the two crystals under strong excitation conditions, we utilized as a pump source a high-brightness, high-power, fiber-coupled diode laser that had a wavelength of 976 nm (bandwidth less than 0.5 nm), a maximum output power of 50 W, a fiber core diameter of 100 μm and a numerical aperture (NA) of 0.22. The pump radiation from the fiber end was first focused by an optical re-imaging unit (ORU) and then was delivered through M1 into the laser crystal, with a pump beam spot radius of about 70 μm. With the help of a calibrated beam splitter, the laser emission spectrum could be monitored by use of a spectrometer, while the output power was measured with a power meter.

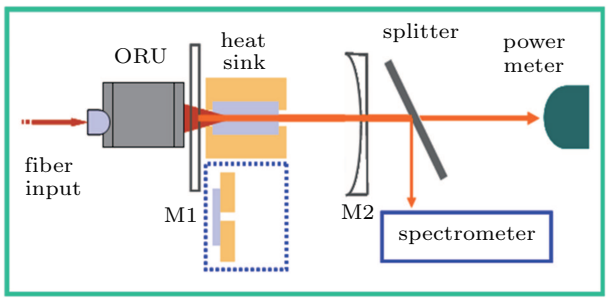


Fig. 1. (color online) Schematic diagram of the experimental setup.

3. Results and discussion

3.1. Comparison of spectroscopic properties

The intrinsic lasing properties of an active ion in a host medium are determined ultimately by its spectroscopic properties in that medium, including absorption spectrum, emission spectrum and fluorescence lifetime (or radiative lifetime). It is therefore necessary to compare the spectroscopic properties of these two crystals, for properly understanding their basic lasing behaviors. The tetragonal $LuPO_4$ and $LuVO_4$ are uniaxial crystals, each with an optic axis along the crystallographic c axis (the four-fold symmetry axis). Consequently, the spectroscopic properties of the Yb ion in these crystals can be fully characterized by two spectra with $\boldsymbol{E} \parallel c$ (π-polarized) and $\boldsymbol{E} \perp c$ (σ-polarized). The fluorescence lifetimes, according to previous work,[10,11] is determined to be 0.256 ms for Yb:$LuVO_4$ and 0.830 ms for Yb:$LuPO_4$.

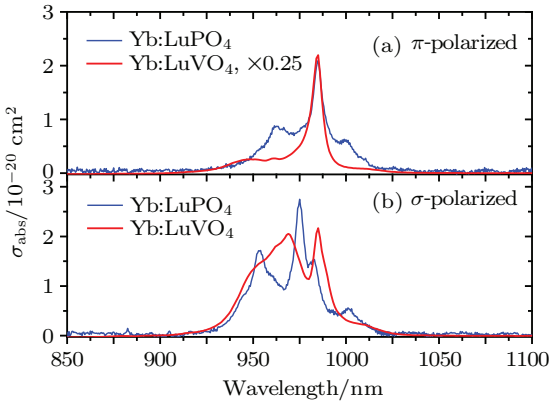


Fig. 2. (color online) (a) π- and (b) σ-polarized absorption cross-section spectra for Yb:$LuPO_4$ and Yb:$LuVO_4$.

Figure 2 shows a direct comparison of polarized absorption cross-section spectra ($\sigma_{abs}(\lambda)$) for the Yb ion in the two crystals, which are measured at room temperature. The π-polarized spectrum for Yb:$LuVO_4$ has been reduced by a factor of 4, in order to facilitate the comparison of spectral features. For the π polarization, the strongest absorptions for both crystals occur at 985.0 nm, corresponding to the zero-phonon transition between the lowest Stark levels of the ground state $^2F_{7/2}$ and the excited state $^2F_{5/2}$. It can be seen that the peak absorption cross-section for Yb:$LuVO_4$ is more than four times greater than that for Yb:$LuPO_4$. In addition to the distinct magnitudes of peak absorption, the spectrum for Yb:$LuVO_4$ is dominated by the zero-phonon transition, whereas for Yb:$LuPO_4$, two additional absorption sidebands centered at 963.4 and 1000.0 nm are also pronounced. For the σ polarization, the absorption spectrum differs largely from that for π polarization, which is true for both crystals, implying the presence of strong anisotropy. In the case of Yb:$LuVO_4$, the maximum absorption still occurs at 985.0 nm (zero-phonon line), but a much wider absorption band, with

its peak located at 969.2 nm, proves to be predominant. For Yb:$LuPO_4$, the absorption spectrum exhibits entirely different features, where the strongest absorption occurs at 975.0 nm and even the short-wavelength sideband peaked at 953.3 nm is also stronger than the zero-phonon absorption at 982.7 nm.

A direct comparison of Yb ion emission spectra ($\sigma_{em}(\lambda)$) in these two host crystals is presented in Fig. 3. Like the absorption spectra, one sees that for the π polarization, the primary emission peaks occurring at 985.0 nm for Yb:$LuPO_4$ and Yb:$LuVO_4$ coincide. However, more features or detailed structures are found in the emission spectrum of Yb:$LuPO_4$, among which the emission bands peaked at about 1000, 1010, 1025 and 1035 nm prove to be of particular importance, because actual laser action is expected to occur within these emission bands. It is worth pointing out that the main emission band around 985 nm, which overlaps the strongest zero-phonon absorption band, is of little significance for practical laser operation due to the existence of extremely high resonant absorption loss. Similarly, for Yb:$LuVO_4$, what turns out to be of practical importance is also the long-wavelength emission sideband covering a range from roughly 1020 to 1055 nm, which will be seen evidently below. The σ-polarized emission spectrum of Yb:$LuVO_4$ consists of a predominant, strongest central band peaked at 985.0 nm, accompanied by two weak short- and long-wavelength sidebands, the latter one being responsible for the actual laser action. In contrast to these characters, the σ-polarized spectrum of Yb:$LuPO_4$ is made up of more separated emission bands, which are peaked at 975.3, 983.1, 1002.0 and 1037.0 nm. The two long-wavelength emission bands prove to relate to the laser action achieved under usual excitation conditions.

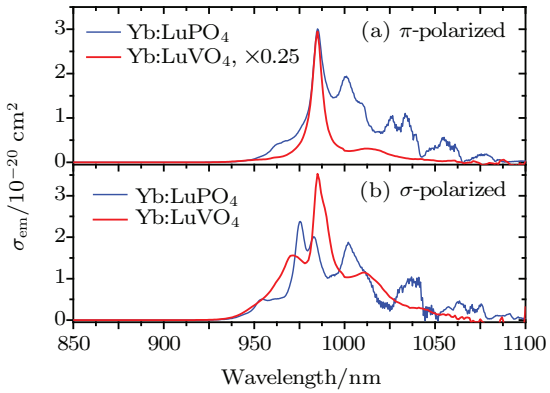


Fig. 3. (color online) (a) π- and (b) σ-polarized emission cross-section spectra for Yb:$LuPO_4$ and Yb:$LuVO_4$.

For a quasi-three-level laser like an Yb ion one, the effective gain cross-section $\sigma_g(\lambda) = \beta\sigma_{em}(\lambda) - (1-\beta)\sigma_{abs}(\lambda)$, with β denoting the fraction of Yb ions that have been excited to the upper manifold ($^2F_{5/2}$), proves to be more useful for evaluating the lasing properties of a laser material. Figure 4 shows a group of $\sigma_g(\lambda)$ curves corresponding to different values of β, calculated for Yb:$LuPO_4$ and Yb:$LuVO_4$.

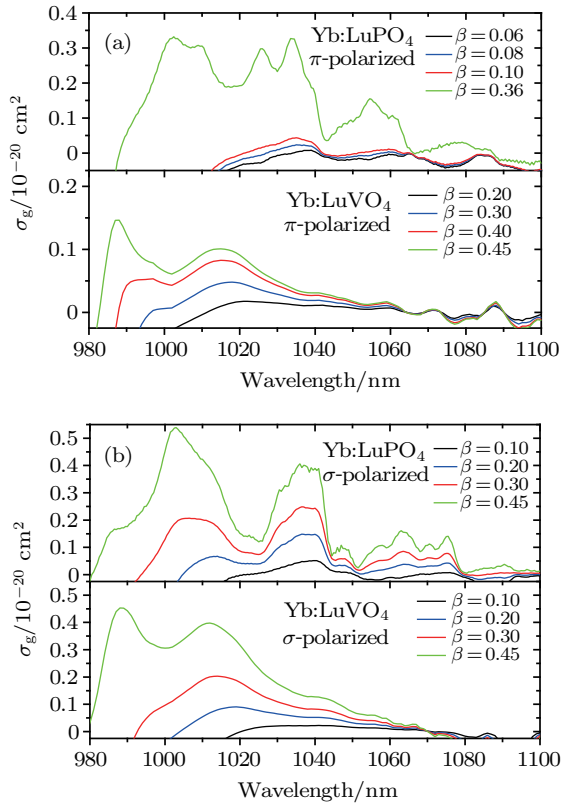


Fig. 4. (color online) (a) π- and (b) σ-polarized gain cross-section curves for Yb:$LuPO_4$ and Yb:$LuVO_4$.

One sees that for the π polarization, the maximum gain cross-section in the case of Yb:$LuVO_4$ shifts toward short-wavelength side with increasing the magnitude of β, and similar behavior is found for Yb:$LuPO_4$ under low excitation levels (small values of β). With the excitation increasing to a sufficiently high level, however, multiple peaks of comparable magnitudes will appear for Yb:$LuPO_4$ crystal as indicated by the curve for $\beta = 0.36$. This implies a severe gain competition. Besides this, it is also seen that under an identical excitation level, the amount of $\sigma_g(\lambda)$ for Yb:$LuPO_4$ is much greater than that for Yb:$LuVO_4$. In contrast to the situation for the π polarization, the σ-polarized maximum gain cross-sections for the two crystals turn out to be quite comparable to each other under the same excitation level.

From the comparison made above, one sees clear distinctions in spectroscopic property between Yb:$LuPO_4$ and Yb:$LuVO_4$ crystals. Considering the same crystal structure and lattice site of Yb ion, such distinctions must be attributed to the differences in the nature of ligand, crystal field strength, covalence effect, electron–phonon interaction, phonon spectrum and density of states.[12]

3.2. Absorption of pump radiation without lasing

To characterize the lasing properties of an active ion in a specific host medium, one needs first to evaluate its capability of absorbing pump radiation. The absorption capability of a sample is usually described by its optical density

O.D. $= 0.434\alpha l$, with α denoting the absorption coefficient and l the sample length.[13] For anisotropic crystals, the magnitude of α depends on the crystal orientation with respect to the pump beam. For the a-cut Yb:$LuVO_4$ or the Yb:$LuPO_4$ plate with pump beam traveling along the a axis, the absorption coefficient for un-polarized pump radiation can be calculated according to $\alpha = [\sigma_{abs}(\pi) + \sigma_{abs}(\sigma)]N_t/2$. For the c-cut Yb:$LuVO_4$ or the Yb:$LuPO_4$ miniature rod with pump beam traveling along the c axis, $\alpha = \sigma_{abs}(\sigma)N_t$. In the expressions N_t is the Yb ion concentration. From Fig. 2, one can read the values for σ_{abs} at the pumping wavelength of 976 nm: for Yb:$LuPO_4$, $\sigma_{abs}(\pi) = 0.85 \times 10^{-20}$ cm^2, $\sigma_{abs}(\sigma) = 2.51 \times 10^{-20}$ cm^2; for Yb:$LuVO_4$, $\sigma_{abs}(\pi) = 2.20 \times 10^{-20}$ cm^2, $\sigma_{abs}(\sigma) = 1.38 \times 10^{-20}$ cm^2. Using these data, one can calculate the values of α and O.D. and the results are listed in Table 1. One can notice that except for the Yb:$LuPO_4$ rod, the values of O.D. for the other three crystal samples are comparable to each other.

Table 1. Parameters relating to absorption of pumping radiation for different crystal samples.

Crystal samples	$N_t/10^{20}$ cm^{-3}	l/cm	α/cm^{-1}	O.D.	η_{a0}	I_{sat}/kW·cm^{-2}
Yb:$LuPO_4$ plate	6.15	0.06	10.33	0.27	0.46	7.62
Yb:$LuPO_4$ rod	6.15	0.2	15.44	1.34	0.95	5.14
Yb:$LuVO_4$, a-cut	1.96	0.2	3.51	0.30	0.50	23.24
Yb:$LuVO_4$, c-cut	1.96	0.2	2.70	0.23	0.42	28.50

We measure the absorption efficiency (η_a), Which is defined as a fraction of incident pump power (P_{in}) absorbed by the sample, over a low power range of $P_{in} < 4.5$ W, for all the crystal samples. The measurement is accomplished under non-lasing conditions by removing the output coupler (M2) from the resonator (Fig. 1). The variations of η_a with P_{in} are illustrated in Fig. 5. The data for Yb:$LuPO_4$ with pump beam $\parallel a$ are measured with the crystal plate, those for pump beam $\parallel c$ are measured with the Yb:$LuPO_4$ miniature rod, while the data for Yb:$LuVO_4$ with pump beam $\parallel a$ or $\parallel c$ are measured with the a- or c-cut crystal samples.

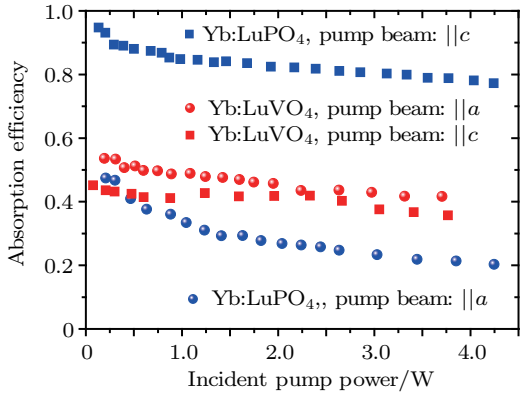


Fig. 5. (color online) Plots of absorption efficiency versus P_{in}, showing their saturation behaviors.

From Fig. 5, one notes first a saturation behavior, i.e., a reduction in the magnitude of η_a with increasing P_{in}. The saturation degrees are different for different samples. At very low level of P_{in} where no saturation occurs, the small-signal or unsaturated absorption efficiency, η_{a0}, can be calculated by $\eta_{a0} = 1 - \exp(-\alpha l)$. Using the parameters given in Table 1, one can calculate the values of η_{a0} for different cases: 0.46 (Yb:$LuPO_4$, pump beam $\parallel a$), 0.95 (Yb:$LuPO_4$, pump beam $\parallel c$), 0.50 (Yb:$LuVO_4$, pump beam $\parallel a$) and 0.42 (Yb:$LuVO_4$, pump beam $\parallel c$). From Fig. 5, one can see good agreement between the measured data and the calculated results. The saturation behavior is characterized by the parameter of absorption saturation intensity (I_{sat}). When the intensity of incident radiation is increased such that I becomes comparable to I_{sat}, the absorption saturation will occur. For a quasi-three-level system like the Yb ion, due to the overlap of absorption and emission spectra, I_{sat} depends on both σ_{abs} and σ_{em} : $I_{sat} = h\nu/(\sigma_{abs} + \sigma_{em})\tau_f$, where τ_f is the fluorescence lifetime and $h\nu$ is the photon energy of the radiation.[14] The value for σ_{abs} at the pumping wavelength (976 nm) has been given above and the emission cross-sections can also been read from Fig. 3: $\sigma_{em}(\pi) = 0.82 \times 10^{-20}$ cm^2, $\sigma_{em}(\sigma) = 2.30 \times 10^{-20}$ cm^2 for Yb:$LuPO_4$; $\sigma_{em}(\pi) = 1.88 \times 10^{-20}$ cm^2, $\sigma_{em}(\sigma) = 1.43 \times 10^{-20}$ cm^2 for Yb:$LuVO_4$. Given the values of $h\nu = 2.05 \times 10^{-19}$ J (pumping wavelength of 976 nm) and $\tau_f = 0.830$ ms (Yb:$LuPO_4$),[11] 0.256 ms (Yb:$LuVO_4$),[10] one can calculate the magnitudes of I_{sat} for different cases and the results are also listed in Table 1. One notes that the saturation intensities for Yb:$LuVO_4$ prove to be much higher than those for Yb:$LuPO_4$, which explains the much less degree of saturation in the absorption of Yb:$LuVO_4$ sample. For the pump beam produced from a fiber-coupled diode laser, its transverse intensity distribution can be assumed to be roughly Gaussian and the on-axis intensity is $I_0 = 2P_{in}/\pi w_p^2$, where w_p is the pump beam spot radius. In our experiment, $w_p = 70$ μm, so that $I_0 \approx 13.0P_{in}$ (kW/cm^2). According to the calculated values for I_{sat} listed in Table 1, one sees that the incident pump power required for causing saturation is roughly 0.5 W (Yb:$LuPO_4$) and 2 W (Yb:$LuVO_4$), which are in agreement with the measurements. From Fig. 5, one may also notice the much more pronounced absorption saturation of Yb:$LuPO_4$ with pump beam $\parallel a$ than that with pump beam $\parallel c$, which is seemingly contrary to the fact that $I_{sat}(\parallel a) > I_{sat}(\parallel c)$ (Table 1). The physical reason for this contradiction is attributed

to the divergence of the pump beam traversing in the crystal sample. In the 2 mm long crystal rod, the beam divergence would be more significant than in the 0.6 mm thick plate, leading to lower intensity away from the beam waist and hence less degree of saturation.

3.3. Lasing properties with an emitting beam along the *a* axis

The lasing properties of the Yb ion in $LuPO_4$ and $LuVO_4$ crystals are investigated, with an emitting laser beam parallel to the *a* or the *c* crystallographic axis. The resonator configuration is optimized individually for each crystal sample. The output characteristics are described in terms of absorbed pump power, which is determined by $P_{abs} = \eta_{a0} P_{in}$. Under lasing conditions, the absorption saturation will greatly diminish because of the presence of intra-cavity circulating laser intensity resulting in stimulated emission from the upper level, giving rise to the so called "population recycling" effect. Due to this effect, the magnitude of η_a could be close to or even reach the value of η_{a0}.[15]

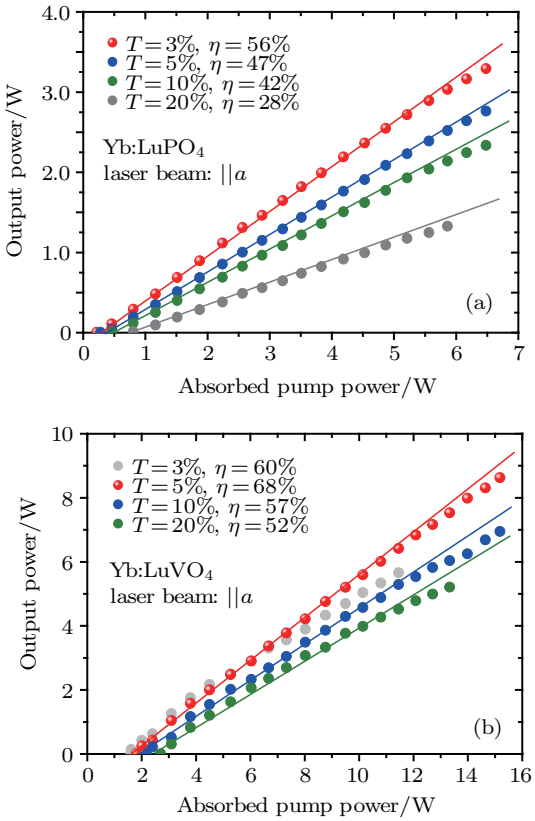


Fig. 6. (color online) Plots of output power versus P_{abs} for different output couplings, generated with emitting laser beam parallel to the *a* axis for (a) $Yb:LuPO_4$ and for (b) $Yb:LuVO_4$.

Firstly, the lasing properties of $Yb:LuPO_4$ with emitting beam $\| a$ are investigated by use of the crystal plate. The optimal laser performance is achieved by employing a resonator of 23 mm in length, which is formed with an output coupler having a curvature radius of 25 mm. Laser action is realized with output coupling ranging from $T = 0.5\%$ to $T = 20\%$, with $T = 3\%$ being optimal. The emitting radiation is linearly polarized with $\boldsymbol{E} \| c$ (π-polarized). Figure 6(a) shows the plots of output power versus P_{abs} for various output couplings. Under the optimal condition of $T = 3$ %, lasing threshold is reached at $P_{abs,th} = 0.22$ W, above which the output power scales linearly with a slope efficiency of 56%, reaching 3.30 W at $P_{abs} = 6.50$ W, the optical–optical conversion efficiency being 50.8%. One sees that even under a relatively high output coupling of $T = 20\%$, fairly efficient laser action can still be achieved, producing an output power of 1.35 W at $P_{abs} = 5.86$ W, the optical–optical and slope efficiencies being 23.0% and 28%, respectively.

We next investigate the lasing properties of $Yb:LuVO_4$ with emitting beam $\| a$ and the crystal sample utilized is the *a*-cut one. In this case, efficient laser action can only be realized with output coupling not greater than $T = 15\%$ and with the resonator ($R_2 = 25$ mm) adjusted in the hemispherical configuration (cavity length of about 26 mm). This seems to be a common character for Yb ion-doped orthovanadate crystal.[3] Figure 6(b) shows the output power as a function of P_{abs} for different output couplings. The polarization state of the emitting laser radiation is also found to be π-polarized. Much higher lasing threshold is observed for $Yb:LuVO_4$ than for $Yb:LuPO_4$. For instance, in the case of $T = 5\%$, which proves to be optimal, the lasing threshold is measured to be $P_{abs,th} = 1.80$ W, in contrast to $P_{abs,th} = 0.28$ W measured under the same output coupling for $Yb:LuPO_4$ (Fig. 6(a)). It should be noted that the results depicted in Fig. 6(b) are obtained in the hemispherical resonator configuration leading to the lowest lasing threshold and the value of $P_{abs,th}$ will even be greatly increased under the same resonator configuration as employed in the case of $Yb:LuPO_4$. The high lasing threshold is believed to be due to the strong resonant absorption loss at the lasing wavelength, which also results in optical bistability.[2] As can be seen in Fig. 6(b), very efficient laser action can be achieved under the optimal output coupling conditions: an output power of 8.63 W is produced at $P_{abs} = 15.2$ W, with an optical–optical conversion efficiency 56.8%. The slope efficiency determined for an pump power range of $P_{in} < 12$ W reaches to 68%. Above this pumping level, the laser action is found to be less efficient, owing to the increasingly strengthened, thermally induced loss.

The lasing wavelengths vary slightly only with pump power increasing, but depend strongly on the output coupling utilized. Figure 7 illustrates the dependence of laser emission spectrum on output coupling for $Yb:LuPO_4$ measured at $P_{abs} = 2.2$ W (Fig. 7(a)) and for $Yb:LuVO_4$ measured at $P_{abs} = 4.1$ W (Fig. 7(b)).

Through a comparison, one can easily recognize the difference in the evolution of lasing wavelength with output cou-

pling between the two crystals. In the case of Yb:$LuPO_4$, the laser emission spectra fall into two separate groups: one with lasing wavelengths ranging from about 1034 to 1042 nm for $T = 5\%$, 3% and 0.5% and the other with lasing wavelengths ranging from about 1009 to 1016 nm for $T = 20\%$ and 10%. In contrast, the laser emission spectrum for Yb:$LuVO_4$ is found to shift progressively, with the output coupling increasing from $T = 0.5\%$ to $T = 15\%$, toward short-wavelength side, from 1051.0–1052.9 nm to 1020.7–1023.2 nm.

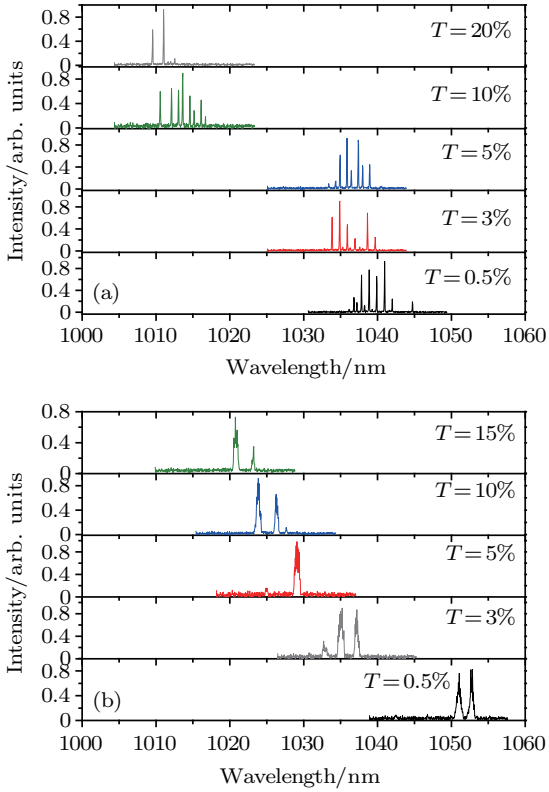


Fig. 7. (color online) Dependence of laser emission spectrum on output coupling for cases with the laser beam parallel to the a axis, measured at (a) $P_{abs} = 2.2$ W for Yb:$LuPO_4$ and (b) $P_{abs} = 4.1$ W for Yb:$LuVO_4$.

The varying behavior of the lasing spectrum with output coupling can be explained qualitatively in accordance with the gain cross-section curves plotted in Fig. 4. For a quasi-three-level laser operating in the free running modes, laser action usually occurs at wavelengths where the effective gain cross-section, and hence the overall gain, reaches its maximum. One sees that for Yb:$LuPO_4$, the maximum values of the π-polarized $\sigma_g(\lambda)$ under low excitation levels of $\beta = 0.06$, 0.08, and 0.10, shift only very slightly, from about 1039 to 1035 nm. This coincides with the variation of lasing spectrum resulting from the output coupling increasing from $T = 0.5\%$ to $T = 5\%$. One can also note that under strong-enough excitation, $\beta \geq 0.36$, the short-wavelength emission band extending from about 1000 to 1010 nm will become dominant. This is the physical reason behind the "jumping" of lasing spectrum when the output coupling is changed from $T = 5\%$ to $T = 10\%$. In the case of Yb:$LuVO_4$, the progressive evolution of lasing spectrum with the output coupling as illustrated in Fig. 7(b), can similarly be understood from the gain maximum shifting with the excitation level. However, the long-wavelength laser emission obtained under low output couplings is not predicted by the $\sigma_g(\lambda)$ curves for small values of β. This disagreement may result from the less accuracy of the emission spectrum in the long wavelength region, which is determined by the reciprocity method and will be severely limited by the extremely low absorption.

3.4. Lasing properties with an emitting beam along the c axis

Laser action with an emitting beam parallel to the crystallographic c axis can be achieved with the Yb:$LuPO_4$ miniature rod or with the c-cut Yb:$LuVO_4$ sample. For Yb:$LuPO_4$, the most efficient laser action is realized by employing a resonator that is formed with a coupler of $R_2 = 15$ mm (cavity length of 13 mm). For Yb:$LuVO_4$, the laser resonator utilized is the same as that in the case of the a-cut sample (a hemispherical cavity). Propagating along the c axis, the laser radiation generated is unpolarized, just as expected, given the fact that the spectroscopic properties for $\boldsymbol{E}$ laying in the plane perpendicular to the optic axis are isotropic.

For the Yb:$LuPO_4$ miniature rod sample, laser action is realized, with output coupling changed from $T = 0.5\%$ to $T = 60\%$. The output characteristics are depicted in Fig. 8(a) for several different output couplings. As long as only the output power and lasing efficiency are concerned, the laser performances prove to be very close to each other for output couplings ranging from $T = 5\%$ to $T = 20\%$ as can be seen in this figure. In the case of $T = 20\%$, the output power increases almost linearly with pump power increasing, with a slope efficiency of 56%. It reaches a maximum value of 8.35 W at $P_{abs} = 17.9$ W, resulting in an optical–optical conversion efficiency of 46.7%. One also sees from Fig. 8(a) that even under an output coupling as high as $T = 60\%$, fairly efficient laser action can still be achieved, with output power approaching nearly a level of 4 W.

As in the case of the a-cut Yb:$LuVO_4$ crystal, laser action is attainable only with the c-cut Yb:$LuVO_4$ sample under output coupling conditions of $T \leq 15\%$. Figure 8(b) shows the output powers versus P_{abs} for different values of T. Once again, one sees much higher lasing thresholds than those for the laser action achieved with the Yb:$LuPO_4$ rod. For example, under the condition of $T = 5\%$, the lasing threshold is measured to be $P_{abs,th} = 1.57$ W, which is twice higher than that for the Yb:$LuPO_4$ rod (0.80 W). The highest output power is generated under an optimal output coupling of $T = 5\%$ and it is measured to be 4.53 W at $P_{abs} = 11.0$ W. The optical–optical conversion efficiency is 41.2%.

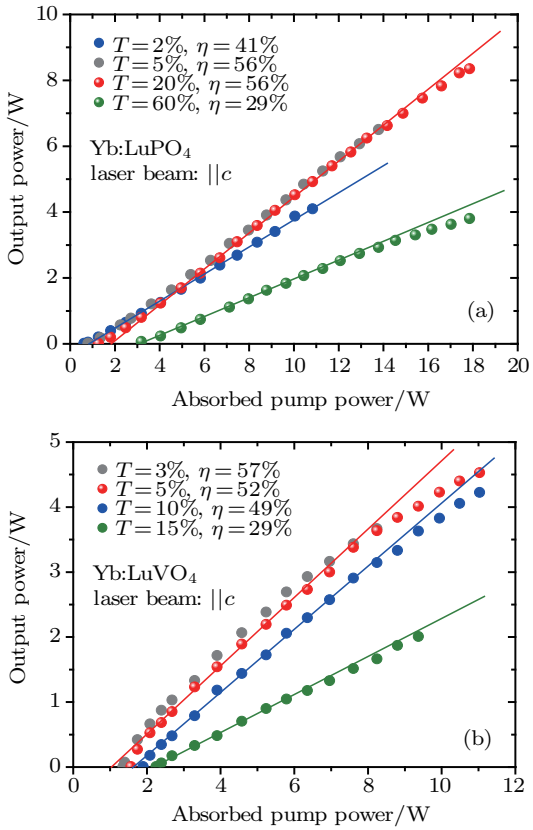


Fig. 8. (color online) Plots of output power versus P_{abs} for different output couplings, generated by an emitting laser beam parallel to the c axis for (a) Yb:$LuPO_4$ and (b) Yb:$LuVO_4$.

In addition to the differences in lasing threshold, output power, and output coupling dependence, the nonlinear natures of the output–input curves for Yb:$LuVO_4$ and Yb:$LuPO_4$ also turn out to be different from each other. One sees from Fig. 8(b) that in particular for lower output couplings, output power increases very rapidly with P_{abs} increasing in the vicinity of lasing threshold, leading to very high local slope efficiency. In contrast, as can be seen in Fig. 8(a) for Yb:$LuPO_4$, the output power just above lasing threshold increases more slowly and the slope efficiency is lower than the value measured at high pump level, a behavior that is typical of most quasi-three-level lasers. Such an anomalous output character results from the unique nature of resonant absorption in Yb:$LuVO_4$ that also leads to bistable laser behavior.[2,16,17]

Figure 9 shows the variations of lasing spectrum with output coupling, measured at $P_{abs} = 8.8$ W for Yb:$LuPO_4$ (Fig. 9(a)) and at $P_{abs} = 3.6$ W for Yb:$LuVO_4$ (Fig. 9(b)). Certain similarities are observed, e.g., the wavelength region over which lasing occurs in the case of $T = 0.5$ % or $T = 5\%$ is seen to be overlapped largely for the two crystals. However, the shortest lasing wavelength attainable for the case of Yb:$LuPO_4$ is found to be within a range of 1000–1005 nm, compared with that of 1015–1020 nm for the case of Yb:$LuVO_4$. As in the case of emitting beam $\parallel a$, the dependence of lasing spectrum on the output coupling can also be understood by referring to the σ-polarized gain cross-section curves depicted in Fig. 4(b).

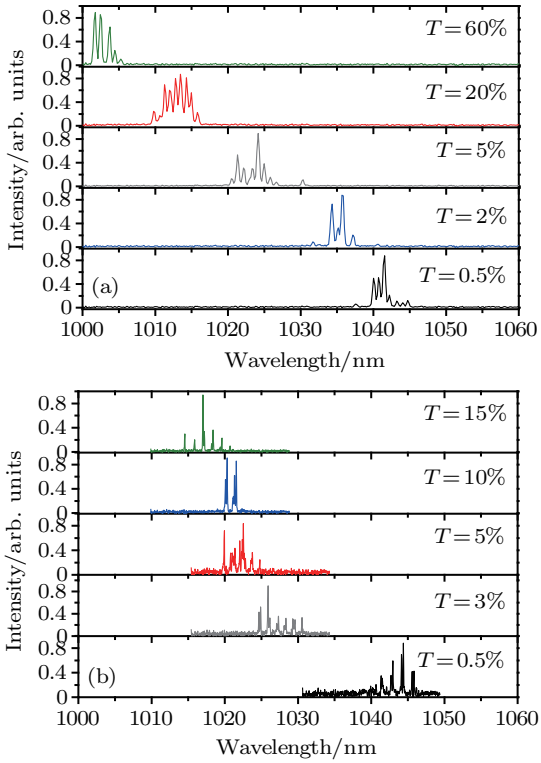


Fig. 9. (color online) Dependence of lasing spectrum on output coupling for the case with the laser beam parallel to the c axis, measured (a) at $P_{abs} = 8.8$ W for Yb:$LuPO_4$ and (b) at $P_{abs} = 3.6$ W for Yb:$LuVO_4$.

3.5. Comparative summary

From the discussion given in the previous subsections, we have seen significant distinctions between Yb:$LuPO_4$ and Yb:$LuVO_4$ in spectroscopic properties, absorption saturation behavior and laser action, despite the fact that they possess the same crystal structure as well as the same local site symmetry for the Yb ion.

The π-polarized absorption or emission spectra of the two crystals share a common feature that they are dominated by the zero-phonon transition band centered at 985.0 nm. However, the peak cross-sections for Yb:$LuVO_4$ are four times greater than for Yb:$LuPO_4$, suggesting much stronger transition strength of Yb ion in $LuVO_4$ crystal. In contrast, the detailed spectral features of either absorption or emission for σ polarization turn out to be entirely different and the peak cross-sections for the Yb ion in the two crystals are comparable to each other.

The absorption for pumping radiation at 976 nm exhibits a considerably different saturation behavior and the degree of saturation proves to be much more pronounced for Yb:$LuPO_4$. This distinction arises from the differences between the two crystals in absorption and emission cross-sections at the pumping wavelength, as well as in fluorescence lifetime.

Some of the lasing properties of the Yb ion in these two host crystals are more or less similar to each other to a certain extent, but many of them turn out to be fairly different.

First of all, only in a hemispherical resonator configuration can the efficient laser action be achieved with Yb:$LuVO_4$. In contrast, efficient laser operation can readily be realized with Yb:LuP O_4 in a common stable resonator. The difficulty in realizing the efficient laser action is believed to be due to the sizable resonant absorption loss existing in Yb:$LuVO_4$ crystal, which is also responsible for the high lasing threshold. Next, the output coupling range, over which laser action could be realized, proves to be much wider for Yb:$LuPO_4$, making it advantageous over Yb:$LuVO_4$ in some applications such as Q-switched lasers. Accompanying this advantage, lasing wavelengths as short as 1000 nm are attainable with Yb:$LuPO_4$. Thirdly, anomalous nonlinearity in the output–input relation is noticed for Yb:$LuVO_4$ with emitting beam $\| c$ and it also results from the unique nature of resonant absorption loss, which can lead to optical bistability in laser action, in particular under very low output coupling.[2,16,17] Such a bistable laser behavior has not been observed with Yb:$LuPO_4$. Very probably, the conditions required for optical bistability to occur, which are determined by the spectroscopic properties,[16,17] cannot be met in Yb:$LuPO_4$. Finally, it is also worth mentioning that experimentally, Q-switching laser action seems to be very difficult to realize with Yb:$LuVO_4$. Until now, little information has been known about passive or active Q-switching laser properties of this crystal. By comparison, both passive and active Q-switching laser action have been demonstrated with Yb:$LuPO_4$.[7–9]

4. Conclusion

We have carried out a comprehensive investigation to compare the lasing properties of the Yb ion in the two tetragonal $LuPO_4$ and $LuVO_4$ isomorphic crystals. Due to the same host crystal structure and identical local site symmetry, a certain degree of similarity is recognized in spectroscopic properties as well as in laser behavior of the Yb ion. On the other hand, however, significantly different spectral features and lasing properties are revealed for the Yb ion doped in the two host crystals. This suggests that, apart from the crystal structure and local site symmetry, other factors may also take crucial roles in determining the spectroscopic and lasing properties, including specific ligand, covalence effect, electron–phonon interaction, density of phonon states and phonon frequency spectrum. In respect of laser performance, the Yb:$LuPO_4$ proves to be superior to Yb:$LuVO_4$, for it enables efficient laser action to be realized much more easily. With a simple plano-concave resonator longitudinally pumped by a 976 nm diode laser, an output power of 3.30 W can be generated from a 0.6 mm thick crystal plate of Yb:$LuPO_4$, whereas the output power attainable from a 2 mm long miniature crystal rod (transverse dimension of 0.7 mm) can reach 8.35 W. These results are rather unusual, showing the great potential of Yb:$LuPO_4$ crystal in making microchips or miniature rod lasers.

References

[1] Yu H, Liu J, Zhang H, Kaminskii A A, Wang Z and Wang J 2014 *Laser Photon. Rev.* **8** 847
[2] Liu J, Petrov V, Griebner U, Noack F, Zhang H, Wang J and Jiang M 2006 *Opt. Express* **14** 12183
[3] Liu J, Han W, Zhang H, Mateos X and Petrov V 2009 *IEEE J. Quantum Elect.* **45** 807
[4] Boatner L A 2002 *Rev. Mineral. Geochem.* **48** 87
[5] Liu J, Han W, Chen X, Zhong D, Teng B, Wang C and Li Y 2014 *Opt. Lett.* **39** 5881
[6] Liu J, Chen X, Han W, Zhong D, Zhang S and Teng B 2015 *Opt. Mater. Express* **5** 2437
[7] Wang L, Dou X, Han W, Xu H, Zhong D, Teng B and Liu J 2017 *Opt. Mater. Express* **7** 1048
[8] Wang L, Han W, Xu H, Zhong D, Teng B and Liu J 2017 *Laser Phys. Lett.* **14** 045807
[9] Dou X, Wang L, Ma Y, Han W, Xu H, Zhong D, Teng B and Liu J 2017 *IEEE Photonics J.* **9** 1503208
[10] Liu J, Mateos X, Zhang H, Wang J, Jiang M, Griebner U and Petrov V 2005 *Opt. Lett.* **30** 3162
[11] DeLoach L D, Payne S A, Chase L L, Smith L K, Kway W L and Krupke W F 1993 *IEEE J. Quantum Elect.* **29** 1179
[12] Henderson B and Imbusch G F 1989 *Optical Spectroscopy of Inorganic Solids* (Oxford: Clarendon Press)
[13] Fox M 2010 *Optical Properties of Solids* (Oxford University Press)
[14] Fan T Y and Byer R L 1987 *IEEE J. Quantum Elect.* **23** 605
[15] Liu J, Han W, Zhang H, Wang J and Petrov V 2008 *Opt. Commun.* **281** 5393
[16] Liu J 2011 *IEEE J. Quantum Elect.* **47** 100
[17] Liu J and Tian X 2013 *IEEE J. Quantum Elect.* **49** 247